2025 American Control Conference (ACC)
July 8-10, 2025. Denver, CO, USA

A Lyapunov-Based Cooperative Adaptive Cruise Control Improving Electric Vehicles Energy Efficiency

Hamed Faghihian[1], Parisa Ansari Bonab[1], Arman Sargolzaei[1]

Abstract— **As the transportation industry increasingly shifts towards electric vehicles (EVs), optimizing energy efficiency becomes crucial due to EVs' ongoing range limitations. Adaptive Cruise Control (ACC) improves driver comfort and safety by maintaining a preset speed and adjusting it to keep safe following distances between EVs. However, ACC tends to be less efficient and slower to react in traffic compared to Cooperative Adaptive Cruise Control (CACC), which leverages vehicle-to-vehicle (V2V) communication for quicker and smoother traffic flow. Therefore, this paper introduces a novel, practical, and energy-efficient Lyapunov-based CACC approach that guarantees safe following distances and facilitates smooth vehicle platooning for EVs. To address the absence of an accurate EV model, we initially performed experimental tests to derive a third-order differential equation representing EV acceleration dynamics and defined a novel controller for it. The proposed controller's performance was then assessed, with an emphasis on energy efficiency and string stability, through both simulations and experimental validation.**

I. Introduction

Adaptive cruise control (ACC) known as a key features of advanced driver assistance systems (ADAS), designed to automatically adjust the speed of a vehicle to ensure a safe distance between vehicles. Cooperative adaptive cruise control (CACC), known as the extension of ACC is made possible through vehicle-to-vehicle (V2V) communication, forming a fundamental part of Connected and Autonomous Vehicles (CAVs) [1]. CACC allows a string of vehicles to follow the lead vehicle with better precision, reduced spacing, and shorter headway times [2], enabling quicker response times and fewer speed fluctuations. These improvements in CACC contribute to enhanced road safety, smoother traffic flow, and lower energy consumption [3]. These features are brought to CACC by transmitting data between vehicles.

Various methodologies employed in the literature to design CACC systems [4–7]. For instance, authors in [4, 5] employed fractional-order adaptive controllers To design CACC. In [8], a set of stochastic linear model predictive control strategies was utilized for CACC. Authors in [7], introduced a Lyapunov-based controller to mitigate the adverse impacts of attacks, external disturbances, and measurement noise in CACC. A critical consideration in CACC design is string stability, which ensures improved distance attenuation, energy efficiency, and safety in a vehicle platoon. However, none of the techniques mentioned above incorporated the analysis of string stability as a crucial factor in ensuring both energy efficiency and robustness.

A string of vehicles is stable if disturbances and fluctuations do not propagate or amplify among downstream vehicles [9, 10]. Consideration of string stability in CACC design studied in the literature [11–13]. For example, [11] proposed a controller design to ensure stability despite time delays. The work reported in [12] used a dynamic information-follow topology to address string stability, The authors in [13] analyzed string stability under potential jamming attacks. While safety and automation are the main goals of CACC, energy efficiency is also crucial. However, none of these designs take energy efficiency into account, and they also aren't specifically developed for EVs.

The impact of CACC on increasing energy efficiency or reducing fuel consumption has been investigated in several studies [14–17]. For instance, [15] shows that CACC can lower fuel consumption by minimizing acceleration and deceleration variations. The effectiveness of CACC in a mixed traffic scenario with both ACC and CACC-equipped vehicles is demonstrated in [18], where the authors show that connectivity-enabled controllers can achieve up to 30% energy savings. Similarly, [14] introduces a real-time, robust eco-CACC system that improves fuel efficiency by up to 23.5%, underscoring its potential to enhance energy efficiency. However, while these studies address various aspects of CACC and string stability, they do not explore how string stability measures affect energy efficiency in CACC systems, particularly for EVs.

Since EVs can utilize regenerative braking for increasing energy efficiency [19], it is necessary to model them differently from vehicles with internal combustion engines when designing an energy-efficient controller. In a recent study [20], an EV model was utilized to ensure string stability, safety, and energy efficiency in CACC. However, the impact of string stability on energy efficiency was not thoroughly analyzed, and a third-order vehicle model was not employed. Using a third-order vehicle model offers a more accurate representation of vehicle dynamics in CACC. Although [21] conducted its analysis using a third-order model, it did not address energy efficiency. Similarly, while the experimental study in [22] used a third-order EV model to assess CACC performance and string stability, energy efficiency was not considered. None of the aforementioned studies explored the integration of a practical EV model in system modeling, nor did they provide a Lyapunov-based CACC approach. Furthermore, the effect of string stability on energy efficiency remains unexamined in the literature.

[1] Hamed Faghihian, Parisa Ansari Bonab, and Arman Sargolzaei are with the Department of Mechanical Engineering, University of South Florida, Tampa, FL 33620, USA. Emails: hfaghihian@usf.edu, parisaansaribonab@usf.edu, a.sargolzaei@gmail.com

In this work, we designed a novel Lyapunov-based CACC system to ensure safety, string stability, and energy efficiency for EVs, considering disturbances and noise. We evaluated the system's performance in both simulations and real-world tests, demonstrating its effectiveness in reducing energy consumption compared to other controllers.

In this paper, the following key contributions presented: (i) Proposing a realistic third-order differential equation model for an EV based on experimental data; (ii) Designing a Lyapunov-based CACC that is easy to implement, robust to external noise and disturbances, enhances energy efficiency, and operates with lower controller gains; (iii) Analyzing the time-domain string stability of the proposed CACC and verifying its advantages through simulations and experiments; (iv) Demonstrating improved energy efficiency by evaluating the impact of string stability on energy consumption.

The layout of this paper structured as: Section II introduces the mathematical model of CACC. Section III outlines the problem statement. The proposed solution is detailed in Section IV and the stability analysis of the proposed controller in Section V. Section VI delivers the results, starting with the experimental analysis for identifying the EV model, followed by evaluations of the proposed CACC's ability to maintain safe and stable distances. Then we presented string stability measure analysis and analysis of total energy consumption. Finally, Section VII provides the conclusion.

II. Mathematical Model of CACC

The schematic of a string of vehicles in a CACC string is shown in Figure 1. For simplicity in the analysis, all vehicles are assumed to be homogeneous. The i^{th} vehicle dynamic model, which came from experimental analysis, modeled as

$$\begin{cases} \dot{x}_i(t) = v_i(t), \\ \dot{v}_i(t) = a_i(t), \\ \dot{a}_i(t) = -\rho_i a_i(t) + \phi_i u_i(t) + d_i(t) + \theta_i(t), \end{cases} \tag{1}$$

where $i \in \{1, \ldots, n\}$ represents the follower vehicle number, in which n representing the total number of vehicles in the string, and the $i-1$ denoting the lead vehicle. Additionally, x_i, v_i, a_i, $u_i \in \mathbb{R}$ represent the position, speed, acceleration, and control input, respectively. Furthermore, $d_i(t) \in \mathbb{R}$ is the external disturbance, and $\theta_i(t) \in \mathbb{R}$ represents measurement noise. The parameters $\rho_i, \phi_i \in \mathbb{R}^+$, with $\mathbb{R}^+$ defined as $\mathbb{R} > 0$, are constants identified through experimental analysis, as explained in Section VI.

Assumption 1. We are assuming that the disturbance is continuous and bounded within a known range. Therefore, we can expect $||d_i(t)|| < \bar{d_1}$, $||d_{i-1}(t)|| < \bar{d_2}$, and $||\dot{d_i}(t)|| < \bar{d_3}$, where $\bar{d_1}, \bar{d_2}, \bar{d_3} \in \mathbb{R}^+$.

Assumption 2. We are assuming that the measurement noise is continuous and bounded within a known range that we can expect that $||\theta_i(t)|| < \bar{\theta_1}$, $||\theta_{i-1}(t)|| < \bar{\theta_2}$ and $||\dot{\theta_i}(t)|| < \bar{\theta_3}$ where $\bar{\theta_1}, \bar{\theta_2}, \bar{\theta_3} \in \mathbb{R}^+$ [23].

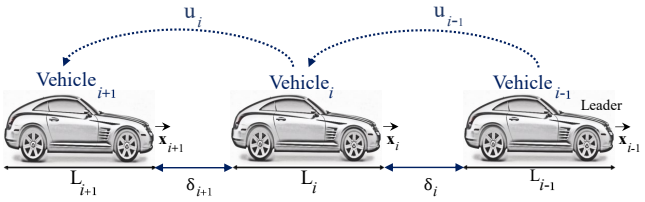

Fig. 1: Illustration of a string of vehicles equipped with CACC.

III. Problem Statement

The CACC platoon, as shown in Figure 1, is assumed to use V2V communication to transmit each vehicle's acceleration command, $u_i(t)$, to its follower, which may be affected by measurement noise, $\theta_i(t)$. The transmission of the acceleration command has been shown to improve both the energy efficiency and the safety of CACC [3]. The vehicle onboard sensors can measure each vehicle acceleration, velocity error, and acceleration error between vehicles. In this section, we are proposing three main objectives for the proposed CACC.

A. Safety

The key objective of the controller design is to maintain a safe distance between vehicles, even in the presence of measurement noise and disturbances. Therefore, the error between desired spacing and actual spacing should remain within a safe range.

B. String Stability

An ideal CACC is responsible for string stability, particularly focusing on the amplification of oscillations down to the string of following vehicles. These oscillations can arise in various contexts, including speed or acceleration errors. According to [24, 25], speed error is a more relevant criterion for assessing string stability. We discuss a method for evaluating the string stability of the proposed CACC and assess its performance through simulation.

C. Energy Efficiency

The CACC must be designed to minimize total energy consumption. Although no direct relationship exists between controller parameters and energy efficiency [19], the designed controller should be verified in terms of its energy performance. Energy efficiency can be evaluated based on the total energy expenditure of each EV in a scenario involving a string of vehicles. Therefore, the third objective is to demonstrate that the proposed method can decrease energy consumption.

IV. Proposed Solution

To quantify the performance of the proposed CACC, we propose the following error signals, auxiliary error signals, and their derivatives.

A. Error Signals

The distance error as the first error signal, defined as $\delta_i(t) \in \mathbb{R}$ as

$$\delta_i(t) = x_{i-1}(t) - x_i(t) - L_{i-1}, \tag{2}$$

where $L_i \in \mathbb{R}$ is the length of the i^{th} vehicle. Additionally, the desired distance between the i^{th} follower and its leader is defined as

$$\delta_{d_i}(t) \triangleq \kappa_1 + \kappa_2 v_i(t), \tag{3}$$

where $\delta_{d_i}(t) \in \mathbb{R}$ represents the desired distance between vehicles, κ_1 is the standstill distance (a constant), and κ_2 is the headway time. Therefore, the distance error $e_i : [t_0, \infty) \to \mathbb{R}$ is defined as

$$e_i(t) \triangleq \delta_i(t) - \delta_{d_i}(t). \tag{4}$$

The following error signals are introduced to facilitate stability analysis

$$\begin{cases} e_{i_1}(t) \triangleq e_i(t), \\ e_{i_2}(t) \triangleq \dot{e}_{i_1}(t), \\ e_{i_3}(t) \triangleq \dot{e}_{i_2}(t), \end{cases} \tag{5}$$

considering (5) and (4), and since $\ddot{v}_i = \dot{a}_i$, therefore

$$e_{i_3}(t) = \ddot{x}_{i-1}(t) - \ddot{x}_i(t) - \kappa_2 \dot{a}_i(t). \tag{6}$$

Using (4), (5) we can write

$$\dot{e}_{i_3}(t) = \dddot{x}_{i-1}(t) - \dddot{x}_i(t) - \kappa_2 \dddot{v}_i(t), \tag{7}$$

using (1) and noting that $\dddot{v}_i = \ddot{a}_i$, we obtain

$$\begin{aligned} \dot{e}_{i_3}(t) = &- \rho_{i-1} a_{i-1}(t) + \phi_{i-1} u_{i-1}(t) \\ &+ \rho_i a_i(t) - \phi_i u_i(t) \\ &- \kappa_2(-\rho_i \dot{a}_i(t) + \phi_i \dot{u}_i(t)) \\ &+ d_{i-1}(t) + \theta_{i-1}(t) \\ &- \big(\kappa_2(\dot{d}_i(t) + \dot{\theta}_i(t)) + d_i(t) + \theta_i(t)\big). \end{aligned} \tag{8}$$

By defining

$$\begin{aligned} \Omega_i(t) \triangleq &d_{i-1}(t) + \theta_{i-1}(t) \\ &- \big(\kappa_2(\dot{d}_i(t) + \dot{\theta}_i(t)) + d_i(t) + \theta_i(t)\big), \end{aligned} \tag{9}$$

we can rewrite (8) as

$$\begin{aligned} \dot{e}_{i_3}(t) = &\phi_{i-1} u_{i-1}(t) - \phi_i(\kappa_2 \dot{u}_i(t) + u_i(t)) \\ &- \rho_{i-1}\big[a_{i-1}(t) - a_i(t) \\ &+ \kappa_2 \rho_i a_i(t) - \kappa_2 \phi_i u_i(t)\big] + \Omega_i(t), \end{aligned} \tag{10}$$

with further simplifications and considering (1), $a_{i-1} = \ddot{x}_{i-1}$, and $a_i = \ddot{x}_i$, we can write (10) as

$$\begin{aligned} \dot{e}_{i_3}(t) = &\phi_{i-1} u_{i-1}(t) - \phi_i(\kappa_2 \dot{u}_i(t) + u_i(t)) \\ &- \rho_{i-1}(\ddot{x}_{i-1}(t) - \ddot{x}_i(t) - \kappa_2(\dot{a}_i(t))) \\ &+ \Omega_i(t), \end{aligned} \tag{11}$$

using (6), yields (11) as

$$\begin{aligned} \dot{e}_{i_3}(t) = &\phi_{i-1} u_{i-1}(t) - \phi_i(\kappa_2 \dot{u}_i(t) + u_i(t)) \\ &- \rho_{i-1} e_{i_3}(t) + \Omega_i(t), \end{aligned} \tag{12}$$

with defining $P_i \triangleq \kappa_2 \dot{u}_i + u_i$, we can write

$$\begin{aligned} \dot{e}_{i_3}(t) = &- \rho_{i-1} e_{i_3}(t) - \phi_i P_i(t) \\ &+ \phi_{i-1} u_{i-1}(t) + \Omega_i(t). \end{aligned} \tag{13}$$

Remark 1. Using Assumptions 1, and 2, we can demonstrate that $||\Omega_i(t)||$ bounded and we can show that $||\Omega_i(t)|| < \bar{\Omega}_i$, where $\bar{\Omega}_i \in \mathbb{R}^+$ is a positive known constant.

To facilitate the design process and stability analysis, two auxiliary error signals $r_{i_1} \in \mathbb{R}$ and $r_{i_2} \in \mathbb{R}$ are defined as

$$\begin{cases} r_{i_1}(t) \triangleq \dot{e}_{i_1}(t) + \alpha_{i_1} e_{i_1}(t), \\ r_{i_2}(t) \triangleq \dot{r}_{i_1}(t) + \alpha_{i_2} r_{i_1}(t), \end{cases} \tag{14}$$

where α_{i_1}, $\alpha_{i_2} \in \mathbb{R}^+$ are known gains, and the method for selecting these gains is introduced in the next section. Additionally, for simplicity of notation, t is omitted in the equations of the following sections.

B. Control Design

Using the defined error signals,we proposed a nonlinear CACC framework based on Lyapunov stability theory. Therefore, the control signal for P_i is derived through the stability analysis outlined in Section V as

$$\begin{aligned} P_i = &e_{i_1}\big[K_i \alpha_{i_1} \alpha_{i_2} + \frac{\alpha_{i_1}^2 \alpha_{i_2} + \alpha_{i_1}}{\phi_i}\big] \\ &+ e_{i_2}\big[K_i \alpha_{i_1} + K_i \alpha_{i_2} + \frac{\alpha_{i_1} \alpha_{i_2} + 1}{\phi_i}\big] \\ &+ e_{i_3}\big[K_i + \frac{\alpha_{i_1} \alpha_{i_2} + 1}{\phi_i}\big], \end{aligned} \tag{15}$$

where $K_i \in \mathbb{R}^+$ is a user-specified gain. Deriving the control signal, u_i, from the definition of P_i and considering (15) as the method for calculating P_i, we can derive the closed loop system which will be used in the stability analysis. To do this, by taking the time derivative of the position error in (14) we can write

$$\dot{e}_{i_1} = r_{i_1} - \alpha_{i_1} e_{i_1}, \tag{16}$$

time derivative of auxiliary errors from (14) are obtained as

$$\begin{cases} \dot{r}_{i_1} = r_{i_2} - \alpha_{i_2} r_{i_1}, \\ \dot{r}_{i_2} = \ddot{r}_{i_1} + \alpha_{i_2} \dot{r}_{i_1}, \end{cases} \tag{17}$$

using (14) and (5) in (17) yields

$$\dot{r}_{i_2} = (\dot{e}_{i_3} + \alpha_{i_1} e_{i_3}) + \alpha_{i_2}(e_{i_3} + \alpha_{i_1} \dot{e}_{i_1}), \tag{18}$$

and substituting (17), yields

$$\dot{r}_{i_2} = \dot{e}_{i_3} + \alpha_{i_1} e_{i_3} + \alpha_{i_2} e_{i_3} + \alpha_{i_2} \alpha_{i_1} r_{i_1} - \alpha_{i_2} \alpha_{i_1}^2 e_{i_1}, \tag{19}$$

substituting $\dot{e}_{i_3}$ from (13) and further simplification yields

$$\begin{aligned} \dot{r}_{i_2} = &e_{i_3}(-\rho_{i-1} + \alpha_{i_1} + \alpha_{i_2}) - \phi_i P_i + \phi_{i-1} u_{i-1} \\ &+ \alpha_{i_2} \alpha_{i_1} r_{i_1} - \alpha_{i_2} \alpha_{i_1}^2 e_{i_1} + \Omega_i(t), \end{aligned} \tag{20}$$

with using P_i from (15) we can write

$$\dot{r}_{i_2} = -K_i \phi_i r_{i_2} - r_{i_1} + \Omega_i(t). \tag{21}$$

The proposed controller ensures a safe distance between vehicles by selecting appropriate gains. Using a third-order model, we directly control acceleration, expecting to result in improved energy efficiency.

C. String Stability Analysis

To address the string stability objective and quantify it, the system is considered string stable if and only if

$$||\zeta_i||_m \leq ||\zeta_{i-1}||_m, \tag{22}$$

where $\zeta_i, \zeta_{i-1} \in \mathbb{R}$ represents the evaluation signal which can be distance error, speed, or acceleration, for the i-th vehicle and its leader, with $||.||_m$ denoting the m-th norm of the signal. As discussed in Section III, the evaluation signal in this study is based on speed. Therefore, the $\mathcal{H}_2$ norm of the string stability criterion, $||\Lambda_i||_2 \in \mathbb{R}$, is defined as:

$$||\Lambda_i||_2 = \frac{||v_i||_2}{||v_{i-1}||_2}. \tag{23}$$

Considering inequality (22), we can write string stability condition as

$$||\Lambda_i||_2 \leq 1, \tag{24}$$

where $2 \leq i \leq n$. Thus, to ensure string stability, it is sufficient to verify this condition for all vehicles in the string, ensuring that fluctuations in upstream traffic do not propagate through the string, which benefits both energy efficiency and traffic flow.

V. Stability Analysis

let $z_i \in \mathbb{R}^3$ be

$$z_i \triangleq [e_{i_1}^T, r_{i_1}^T, e_{i_2}^T]. \tag{25}$$

Let the following be the sufficient conditions for the stability analysis

$$\alpha_{i_2} > \frac{\varepsilon_{1_i}}{2}, \qquad \alpha_{i_1} > \frac{1}{2\varepsilon_{1_i}}, \qquad K_i > \frac{1}{2\varepsilon_{2_i}\phi_i}, \tag{26}$$

where $\varepsilon_{1_i} \in \mathbb{R}^+$ denotes a positive known constant. Also, let consider $\nu_i \triangleq \min\{\alpha_{i_1}, \alpha_{i_2}, \phi_i\}$.

Theorem 1. *For the dynamic system introduced in* (1)*, the controller given in* (15) *ensures semi-globally uniformly ultimately bounded (UUB) of the tracking error such that*

$$\lim_{t\to\infty} \sup ||z_i(t)|| \leq \frac{\varepsilon_{2_i}}{2}\bar{\Omega}_i. \tag{27}$$

Proof: Let $V_i \in \mathbb{R}^3$ be a positive definite, continuously differentiable Lyapunov function defined as

$$V_i = \frac{1}{2}e_{i_1}^2 + \frac{1}{2}r_{i_1}^2 + \frac{1}{2}r_{i_2}^2, \tag{28}$$

Defining $\lambda_{i_1}, \lambda_{i_2} \in \mathbb{R}$ as

$$\lambda_{i_1} \triangleq \max\left\{-\alpha_{i_2} + \frac{\varepsilon_{1_i}}{2}, -\alpha_{i_1} + \frac{1}{2\varepsilon_{1_i}}, \frac{1}{2\varepsilon_{2_i}} - K_i\phi_i\right\}, \tag{29}$$

$$\lambda_{i_2} \triangleq \frac{\varepsilon_{2_i}}{2}\bar{\Omega}_i. \tag{30}$$

The function V_i in (28) is a bounded Lyapunov candidate function, such that

$$\chi_{i_1} \leq V_i \leq \chi_{i_2}, \tag{31}$$

where, $\chi_{i_1} \triangleq \frac{\lambda_{i_1}}{\lambda_{i_2}}$, and $\chi_{i_2} \triangleq \frac{2\lambda_{i_1}}{\lambda_{i_2}}$.

To prove Theorem 1, we first take the time derivative of the Lyapunov function, (28), which gives

$$\dot{V}_i = e_{i_1}\dot{e}_{i_1} + r_{i_1}\dot{r}_{i_1} + r_{i_2}\dot{r}_{i_2}, \tag{32}$$

using time derivatives of all errors in (16), (17), and (21) we have

$$\begin{aligned}\dot{V}_i =& e_{i_1}(r_{i_1} - \alpha_{i_1}e_{i_1}) + r_{i_1}(r_{i_2} - \alpha_{i_2}r_{i_1}) \\ &+ r_{i_2}(-K_i\phi_i r_{i_2} - r_{i_1} + \Omega_i),\end{aligned} \tag{33}$$

simplification of (33) gives

$$\dot{V}_i = -\alpha_{i_2}r_{i_1}^2 - K\phi_i r_{i_2}^2 - \alpha_{i_1}e_{i_1}^2 + e_{i_1}r_{i_1} + +r_{i_2}\Omega_i, \tag{34}$$

the following inequality can be held for (34) as

$$\begin{aligned}\dot{V}_i \leq& -\alpha_{i_2}\left\|r_{i_1}\right\|^2 - K_i\phi_i\left\|r_{i_2}\right\|^2 - \alpha_{i_1}\left\|e_{i_1}\right\|^2 \\ &+ \left\|e_{i_1}\right\|\left\|r_{i_1}\right\| + \left\|r_{i_2}\right\|\left\|\Omega_i\right\|.\end{aligned} \tag{35}$$

Young's Inequality is employed to handle specific terms in (35), and by using Remark 1 we can conclude

$$\begin{aligned}\left\|e_{i_1}\right\|\left\|r_{i_1}\right\| &\leq \frac{1}{2\varepsilon_{1_i}}\left\|e_{i_1}\right\|^2 + \frac{\varepsilon_{1_i}}{2}\left\|r_{i_1}\right\|^2, \\ \left\|r_{i_2}\right\|\left\|\Omega_i\right\| &\leq \frac{1}{2\varepsilon_{2_i}}\left\|r_{i_2}\right\|^2 + \frac{\varepsilon_{2_i}}{2}\bar{\Omega}_i^2,\end{aligned} \tag{36}$$

using (36), the inequality in (35) can be written as

$$\begin{aligned}\dot{V}_i \leq& -\alpha_{i_2}\left\|r_{i_1}\right\|^2 - K_i\phi_i\left\|r_{i_2}\right\|^2 - \alpha_{i_1}\left\|e_{i_1}\right\|^2 \\ &+ \frac{1}{2\varepsilon_{1_i}}\left\|e_{i_1}\right\|^2 + \frac{\varepsilon_{1_i}}{2}\left\|r_{i_1}\right\|^2 + \frac{1}{2\varepsilon_{2_i}}\left\|r_{i_2}\right\|^2 + \frac{\varepsilon_{2_i}}{2}\bar{\Omega}_i^2.\end{aligned} \tag{37}$$

Simplifying (37) results

$$\begin{aligned}\dot{V} \leq& (-\alpha_{i_2} + \frac{\varepsilon_{1_i}}{2})\left\|r_{i_1}\right\|^2 + (-\alpha_{i_1} + \frac{1}{2\varepsilon_{1_i}})\left\|e_{i_1}\right\|^2 \\ &(\frac{1}{2\varepsilon_{2_i}} - K\phi_i)\left\|r_{i_2}\right\|^2 + \frac{\varepsilon_{2_i}}{2}\bar{\Omega}_i^2.\end{aligned} \tag{38}$$

Satisfying the sufficient conditions in (26) yields

$$\dot{V}_i \leq -\lambda_{i_1}\left\|z_i\right\|^2 + \lambda_{i_2}. \tag{39}$$

Given that the Lyapunov candidate function in (28) is bounded according to the inequality in (31), the inequality in (39) is upper-bounded and can be used to calculate the upper bound expressed in (27). Based on this, we can show By designing the controller is derived from (15), z_i is bounded, which ultimately leads to $e_{i_1}, r_{i_1}, r_{i_2}$ belong to the space L_∞, which means they remain bounded for all time.

VI. Results

In the results section, we first present the EV model derivation, followed by simulation and experimental results assessing CACC performance. We then evaluate the string stability and energy efficiency of the proposed controller.

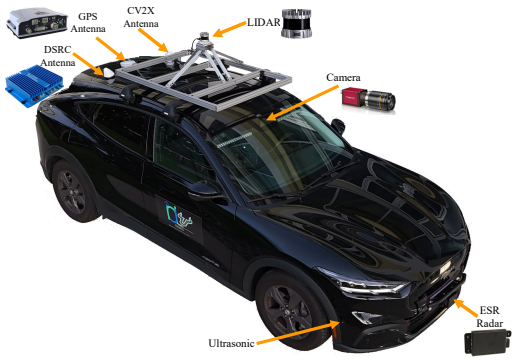

Fig. 2: The EV is used for experimental analysis.

A. *Vehicle Model Through Experimental Analysis*

To provide an accurate and realistic EV model, the transfer function obtained through experiments using the a Mustang Mach-E (Figure 2). The desired acceleration sent as command, and the actual acceleration measured with the vehicle on-board sensors.

Therefore, considering the vehicle's longitudinal dynamics as a first-order system, the transfer function is

$$T_i(s) = \frac{\phi_i}{s + \rho_i}, \tag{40}$$

where $\rho_i \triangleq \frac{1}{\tau_i}$, with $\tau_i \in \mathbb{R}$ as the vehicle time constant, and $\phi_i \in \mathbb{R}$ can be found as

$$\phi_i = \rho_i \frac{a_{i_{ss}}}{u_{i_{ss}}}, \tag{41}$$

where $a_{i_{ss}} \in \mathbb{R}$ is the steady-state measured acceleration, and $u_{i_{ss}} \in \mathbb{R}$ is the steady-state desired acceleration. We repeated the test 25 times with varying acceleration commands ranging from $0.1\ m/s^2$ to $1\ m/s^2$. The average of all measured accelerations, scaled to unit acceleration for averaging, shown in Figure 3. Based on Figure 3, the first-order transfer function model of the vehicle is

$$T_i(s) = \frac{0.73779}{s + 0.6998}. \tag{42}$$

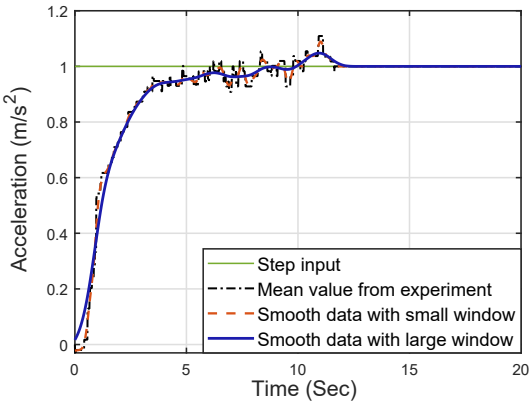

Fig. 3: Obtained experimental step response for acceleration.

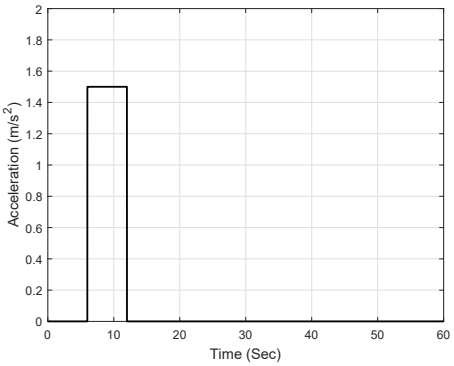

Fig. 4: Desired acceleration input for the lead vehicle in the scenario 1.

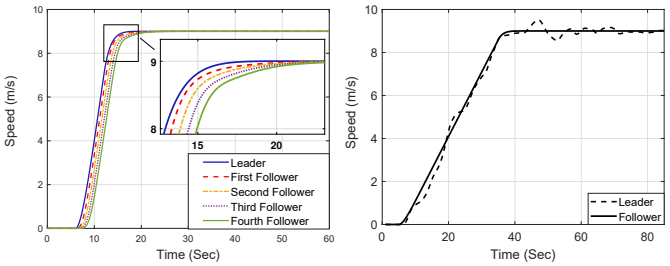

(a) (b)

Fig. 5: Speed profiles for CACC evaluation: (a) Simulation with 4 followers, (b) Experimental result for leader and first follower.

B. *CACC Performance Evaluation*

The controller was tested in both simulations and experiments. To assess its safety measures, the vehicle string subjected to a sudden acceleration command change of the lead vehicle from 0 to 1.5 m/s^2, followed by a rapid decrease to zero within 5 seconds, as shown in Figure 4.

Testing different headway times showed that 0.5 seconds is the minimum needed to ensure minimal fluctuation among followers. The speed profile of the leader and all four followers in the simulation environment shown in figure 5.a. As depicted, The designed controller compensates for speed and acceleration changes without introducing fluctuations within five vehicles. To verify, we conducted an experimental test using the same EV introduced in Section VI-A as the first follower. The speed comparison between the first follower and the leader is shown in Figure 5.b, with experimental results consistent with simulations. The root mean square error (RMSE) for the position is provided in Table I. However, the RMSE presented in Table I demonstrates the effectiveness of the designed controller in the experiment. The difference between simulation and experimental RMSE arises from

TABLE I: Average of position RMSE in CACC performance evaluation.

Configuration	Position RMSE
Simulation,	0.0632
Experiment,	0.8545

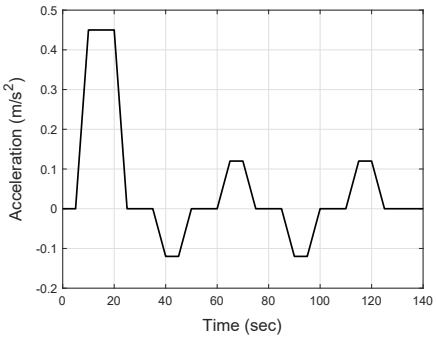

Fig. 6: Desired acceleration of the lead vehicle for energy efficiency and string stability tests.

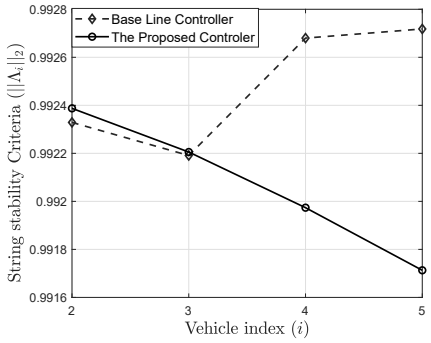

Fig. 8: Comparison of time-domain string stability criteria between the proposed and baseline controllers.

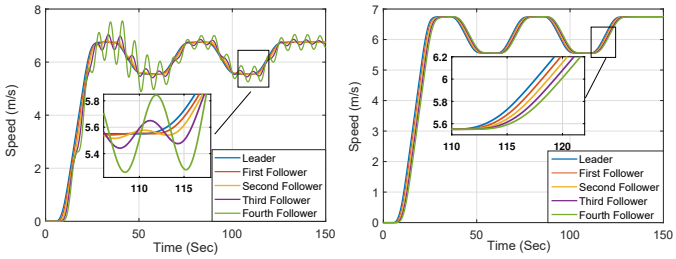

(a) (b)

Fig. 7: Simulation results of speed profiles for a string of five vehicles with (a) The baseline controller. (b) The proposed controller.

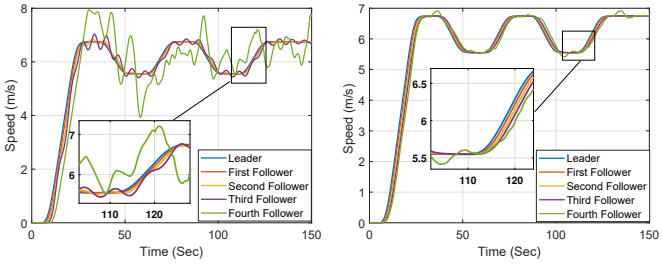

(a) (b)

Fig. 9: Results of speed profiles for a string of five vehicles in the experiment with (a) The baseline controller. (b) The proposed controller.

limitations in practical implementation and measurement constraints, yet it remains within an acceptable range for experiments.

C. *Energy Efficiency and String Stability Evaluation*

A drive cycle for the lead vehicle, shown in Figure 6, was used to evaluate the proposed controller's impact on energy efficiency and string stability. The cycle is based on the ECE-15 drive cycle, known for assessing energy efficiency under demanding conditions [26]. The standard drive cycle is modified to test both high- and low-speed segments, making it suitable for CACC testing, especially for EVs benefiting from regenerative braking systems. This setup allows for a comprehensive assessment of energy efficiency and string stability under varied driving conditions.

A baseline PID-based CACC was used to compare the designed controller's effects on string stability and energy efficiency. A combination of simulations and experiments was employed to assess both metrics. The comparison of the speed profiles of five vehicles in the simulation environment is shown in Figure 7, demonstrating how the proposed controller can reduce speed fluctuations.

String stability was analyzed for both controllers, as shown in Figure 8. In the proposed controller, the string stability criteria decrease along the vehicle string, while the baseline controller shows an increase, demonstrating that a controller designed to minimize all errors $(e_{i_1}, e_{i_2}, e_{i_3})$ is more effective in enhancing string stability than one focused only on eliminating distance error, e_{i_1}.

In the experimental setup, the first four vehicles modeled in the simulated environment, while the the fifth vehicle in the string was the experimental EV described in Section VI-A, which shaped the vehicle-in-the-loop setup. The comparison of speed profiles for five vehicles in the combined simulation and experimental environment is shown in Figure 9, demonstrating how the proposed controller reduces speed fluctuations, as verified by experimental results for the last vehicle in the string.

Power data was collected in experiments to evaluate energy consumption where the real EV was used as the last vehicle in a string of five, with both the proposed and baseline controllers. Figure 10 shows this comparison.

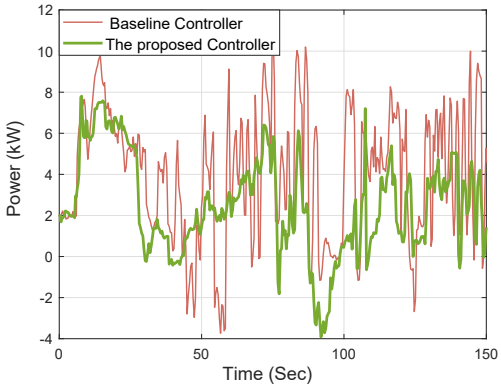

Fig. 10: Comparison of power EV power data between the proposed controller and the baseline controller.

The comparison between total energy consumption and time-domain string stability criteria for both controllers is shown in Table II. The results demonstrate how our controller's improved string stability reduces energy consumption by up to 39%.

TABLE II: Comparison of average time-domain string stability criteria and total energy consumption between the proposed and baseline controllers

Controller	Average time-domain string stability criteria	Overall energy consumed (KJ)
Proposed controller	0.9921	403.03
Baseline controller	0.9925	671.17

VII. Conclusion

In this paper, we proposed a practical Lyapunov-based control method to increase the energy efficiency of the CACC algorithm. We demonstrated that the controller effectively stabilized a string of vehicles in both simulations and experiments. This work presented a practical approach to designing a CACC.

We showed that employing Lyapunov stability to ensure that distance, velocity, and acceleration errors converged to zero together, even in the presence of noise and disturbances, improved string stability, enabled smoother speed transitions, and increased energy efficiency. These benefits are particularly important for EVs, where smooth driving improves the effectiveness of regenerative braking, leading to higher energy efficiency.

VIII. Acknowledgement

Partial support for this research was provided by the National Science Foundation under Grant No. ECCS-EPCN-2241718. Any opinions, findings, conclusions, or recommendations expressed in this material are those of the author(s) and do not necessarily reflect the views of the sponsoring agency.

References

[1] H. Faghihian, J. Holland, and A. Sargolzaei, "Chapter 1 - introduction to autonomous vehicles," in *Handbook of Power Electronics in Autonomous and Electric Vehicles* (M. H. Rashid, ed.), pp. 1–16, Academic Press, 2024.

[2] K. C. Dey, L. Yan, X. Wang, Y. Wang, H. Shen, M. Chowdhury, L. Yu, C. Qiu, and V. Soundararaj, "A review of communication, driver characteristics, and controls aspects of cooperative adaptive cruise control (cacc)," *IEEE Transactions on Intelligent Transportation Systems*, vol. 17, no. 2, pp. 491–509, 2015.

[3] H. Faghihian and A. Sargolzaei, "Energy efficiency of connected autonomous vehicles: A review," *Electronics*, vol. 12, no. 19, p. 4086, 2023.

[4] H. Balaska, S. Ladaci, H. Schulte, and A. Djouambi, "Adaptive cruise control system for an electric vehicle using a fractional order model reference adaptive strategy," *IFAC-PapersOnLine*, vol. 52, no. 13, pp. 194–199, 2019.

[5] H. Bouyedda, S. Ladaci, and H. Schulte, "Cruise control design for an electric vehicle using a fractional order pi λ d μ with genetic algorithms optimization," in *2019 8th International Conference on Systems and Control (ICSC)*, pp. 158–163, IEEE, 2019.

[6] F. J. Niroumand, P. A. Bonab, and A. Sargolzaei, "Security of connected and autonomous vehicles: A review of attacks and mitigation strategies," *SoutheastCon 2024*, pp. 1197–1204, 2024.

[7] P. Ansari-Bonab, J. C. Holland, J. Cunningham-Rush, S. Noei, and A. Sargolzaei, "Secure control design for cooperative adaptive cruise control under false data injection attack," *IEEE Transactions on Intelligent Transportation Systems*, 2024.

[8] D. Moser, H. Waschl, H. Kirchsteiger, R. Schmied, and L. del Re, "Cooperative adaptive cruise control applying stochastic linear model predictive control strategies," in *2015 European Control Conference (ECC)*, pp. 3383–3388, 2015.

[9] J. Wang, Y. Zheng, C. Chen, Q. Xu, and K. Li, "Leading cruise control in mixed traffic flow: System modeling, controllability, and string stability," *IEEE Transactions on Intelligent Transportation Systems*, vol. 23, no. 8, pp. 12861–12876, 2021.

[10] A. Corli and H. Fan, "String stability in traffic flows," *Applied Mathematics and Computation*, vol. 443, p. 127775, 2023.

[11] U. Montanaro, M. Tufo, G. Fiengo, M. di Bernardo, A. Salvi, and S. Santini, "Extended cooperative adaptive cruise control," in *2014 IEEE Intelligent Vehicles Symposium Proceedings*, pp. 605–610, IEEE, 2014.

[12] S. Gong, A. Zhou, and S. Peeta, "Cooperative adaptive cruise control for a platoon of connected and autonomous vehicles considering dynamic information flow topology," *Transportation research record*, vol. 2673, no. 10, pp. 185–198, 2019.

[13] A. Alipour-Fanid, M. Dabaghchian, H. Zhang, and K. Zeng, "String stability analysis of cooperative adaptive cruise control under jamming attacks," in *2017 IEEE 18th International Symposium on High Assurance Systems Engineering (HASE)*, pp. 157–162, IEEE, 2017.

[14] Y. Shao and Z. Sun, "Robust eco-cooperative adaptive cruise control with gear shifting," in *2017 American Control Conference (ACC)*, pp. 4958–4963, IEEE, 2017.

[15] I. Mahdinia, R. Arvin, A. J. Khattak, and A. Ghiasi, "Safety, energy, and emissions impacts of adaptive cruise control and cooperative adaptive cruise control," *Transportation Research Record*, vol. 2674, no. 6, pp. 253–267, 2020.

[16] X. Chen, J. Yang, C. Zhai, J. Lou, and C. Yan, "Economic adaptive cruise control for electric vehicles based on adhdp in a car-following scenario," *IEEE Access*, vol. 9, pp. 74949–74958, 2021.

[17] Y. Zhang, Y. Bai, M. Wang, and J. Hu, "Cooperative adaptive cruise control with robustness against communication delay: An approach in the space domain," *IEEE Transactions on Intelligent Transportation Systems*, vol. 22, no. 9, pp. 5496–5507, 2020.

[18] M. Shen, R. A. Dollar, T. G. Molnar, C. R. He, A. Vahidi, and G. Orosz, "Energy-efficient reactive and predictive connected cruise control," *IEEE Transactions on Intelligent Vehicles*, vol. 9, no. 1, pp. 944–957, 2023.

[19] H. Faghihian, M. Sarkar, and A. Sargolzaei, "A novel energy-efficient regenerative braking system for electric vehicles," in *SoutheastCon 2024*, pp. 1300–1305, 2024.

[20] J. Li, C. Chen, B. Yang, J. He, and X. Guan, "Energy-efficient cooperative adaptive cruise control for electric vehicle platooning," *IEEE Transactions on Intelligent Transportation Systems*, 2023.

[21] H. Xing, J. Ploeg, and H. Nijmeijer, "Robust cacc in the presence of uncertain delays," *IEEE Transactions on Vehicular Technology*, vol. 71, no. 4, pp. 3507–3518, 2022.

[22] T. Ogitsu and M. Omae, "Experimental testing of cooperative adaptive cruise control using small electric vehicles," *Journal of the Institute of Industrial Applications Engineers*, vol. 4, no. 3, pp. 118–121, 2016.

[23] P. A. Bonab and A. Sargolzaei, "A nonlinear control design for cooperative adaptive cruise control with time-varying communication delay," *Electronics*, vol. 13, no. 10, 2024.

[24] C. Lei, E. Van Eenennaam, W. K. Wolterink, G. Karagiannis, G. Heijenk, and J. Ploeg, "Impact of packet loss on cacc string stability performance," in *2011 11th International Conference on ITS Telecommunications*, pp. 381–386, IEEE, 2011.

[25] R. Pueboobpaphan and B. V. Arem, "Driver and vehicle characteristics and platoon and traffic flow stability: Understanding the relationship for design and assessment of cooperative adaptive cruise control," *Transportation Research Record*, vol. 2189, no. 1, pp. 89–97, 2010.

[26] EuroMotor Virtual College, "ECE-City Driving Cycle for Manual Transmission Vehicles," 2022. ([Online]. https://www.euromotor.org/mod/resource/view.php?id=21265 (Accessed on: 2024, September 27).